Materials Science and Engineering C 75 (2017) 845–853

Contents lists available at ScienceDirect

Materials Science and Engineering C

journal homepage: www.elsevier.com/locate/msec

Fabrication of polypropylene/silver nanocomposites for biocidal applications

Washington Luiz Oliani [a,*], Duclerc Fernandes Parra [a], Luiz Gustavo Hiroki Komatsu [a], Nilton Lincopan [b,c], Vijaya Kumar Rangari [d], Ademar Benevolo Lugao [a]

[a] Nuclear and Energy Research Institute, IPEN-CNEN/SP, Av. Prof. Lineu Prestes, 2242 – Cidade Universitária – CEP, 05508-000 São Paulo, Brazil
[b] Department of Microbiology, Institute of Biomedical Sciences, University of Sao Paulo, 05508-000, São Paulo, Brazil
[c] Department of Clinical Analysis, School of Pharmacy, University of São Paulo, 05508-000, São Paulo, Brazil
[d] Department of Materials Science and Engineering, Tuskegee University, AL 36088, USA

ARTICLE INFO

Article history:
Received 25 November 2016
Received in revised form 19 December 2016
Accepted 21 February 2017
Available online 27 February 2017

ABSTRACT

This paper presents a study on biocidal effect of polymer nanocomposite films of gamma irradiated polypropylene (PP) and silver nanoparticles. The modified polypropylene was obtained from isotactic polypropylene (iPP) in pellets form by irradiation with gamma rays in the presence of acetylene. A new morphology with long chain branching of PP and distinct rheology is obtained by this process. The blend of 50/50 wt% neat PP and PP modified by gamma radiation were further mixed using a twin screw extruder. The AgNPs were infused into this polymer blend at different concentrations of: 0.1%; 0.25%; 0.5%; 1.0%; 1.0% (PVP), 2.0% and 4.0% by wt%. These polymer nanocomposites were characterized by Raman spectroscopy, scanning electron microscopy (SEM), energy dispersive spectroscopy (EDS), thermogravimetric analysis (TG), differential scanning calorimetry (DSC), X-ray diffraction (XRD), transmission electron microscopy (TEM), cytotoxicity test and Kirby-Bauer disk diffusion techniques. The bactericidal effect of *Pseudomonas aeruginosa* (*P. aeruginosa*) and *Staphylococcus aureus* (*S. aureus*) were assessed in detail.

1. Introduction

Polypropylene (PP) has emerged as an environmentally friendly polymeric material because its low cost and high chemical resistance coupled with ease of fabrication, high versatility in applications and recycling [1,2]. PP is the fastest growing commodity resin in the thermoplastic polymers world market [3].

PP has low melt strength, low elasticity, and a narrow processing window because of its linear macromolecular architecture and semi-crystalline nature. As a result, upon heating PP to its melting temperature, it undergoes sharp transition from a semi crystalline solid to a melt that has no appreciable rubbery plateau. Hence, PP cannot be easily used in melt processing operations such as deep draw thermoforming, upward film blowing and extrusion coating, which involve free surfaces undergoing extensional deformation [3–5].

An effective approach to achieve high-melt-strength-polypropylene (HMSPP) is to add long-chain-branches (LCB) into linear PP, onto backbone, using gamma radiation and acetylene. The grafting and branching result from macroradicals combinations during the irradiation process [6–9]. The strain hardening effect of the HMSPP represents an important role in many processing operations like film blowing, blow molding, foam expansion, fiber spinning and thermoforming [10].

Extrusion process has been one of the important basic processing technologies for producing polymer based compounds. The extrusion technology has been divided into two major streams. The first stream goes towards higher efficiency using lager scale processing lines, and the other towards the production of functional products with special properties, such as nanocomposites and/or polymer blends with specified nanoscale morphology [11].

The modification of polypropylene with inorganic nanoparticles (AgNPs) nanocomposites prepared by melt mixing may provide some functionality to the polymer. Applications such as household, automotive, and packaging materials depend on the properties of the inorganic nanoparticles. The presence of Ag nanoparticles increases the crystallization temperature of iPP even at very low Ag content, which represents a high efficiency of the heterogeneous nucleation [12,13]. The dispersion of particle agglomerates is a key processing step in many industrial applications. Solid particle clusters are subjected to shearing forces while flowing through the process streams. They are broken down into smaller components and are distributed [14]. Although the properties of the dispersing fluid and the particulate material can be very diverse, depending on the application, the same fundamental principles are apply to control the dispersion process and the properties of the

* Corresponding author.
E-mail address: washoliani@usp.br (W.L. Oliani).

http://dx.doi.org/10.1016/j.msec.2017.02.109
0928-4931/

Table 1
Samples of PP-nanocomposites with addition AgNPs (wt%).

Sample	A	B	C	D	E	F	G	H
PPAgNPs/wt%	PP0	PP0.1	PP0.25	PP0.5	PP1.0	PP1.0PVP	PP2.0	PP4.0

*HMSPP obtained at 12.5 kGy was used as control: PP0.

final product [15]. In spite of antimicrobial activity, active substances can be incorporated directly into polymeric materials or previously encapsulated by organic coating for follow polymer incorporation.

Thermal processing such as melt blending, extrusion and injection molding have also been applied to incorporate the antimicrobials into polymers. The thermal stability of active component and chemical compatibility of polymer matrix and antimicrobials should be considered in order to evenly distribute antimicrobial substance [16]. Silver is particularly attractive because its high toxicity against bacteria at exceptionally low concentrations and a very low toxicity for humans [17,18].

Colloidal silver and silver nanoparticles are increasingly used as antimicrobial agents, stimulated by its depot function for silver ions and its high specific surface area [19].

Recently, silver nanoparticles (AgNPs), metallic silver obtained in nanosize are stabilized with different surfactants such as, polyvinyl pyrrolidone (PVP) or oleic acid (OA) for better dispersion [20].

These polypropylene-AgNPs compounds were prepared by melt mixing, and the effects of the processing conditions on nanoparticles dispersion were investigated, as well as, antimicrobial properties of polypropylene filled with coated AgNPs [20].

The mechanisms behind the activity of nano-scaled silver on bacteria are not fully elucidated yet. The three most common mechanisms of toxicity proposed to date are: (1) uptake of free silver ions followed by disruption of ATP production and DNA replication, (2) silver nanoparticles and silver ion generation of ROS, and (3) direct damage to cell membranes by silver nanoparticles [21–23].

In our recent study we developed a method for branched PP, based on the grafting of long chain branches on PP backbone using acetylene as a crosslink promoter under gamma radiation process [24]. In the current study we extended the branched PP to incorporate AgNPs. Films of polypropylene nanocomposite with silver nanoparticles were obtained by extrusion process and evaluated for biocidal effect of bacteria *P. aeruginosa* and *S. aureus*.

2. Experimental

2.1. Materials

The isotactic Polypropylene (iPP) with MFI = 1.5 dg min^{-1} and Mw = 338,000 g mol^{-1} from Braskem – Brazil, was supplied in pellets. Acetylene 99.8% supplied by White Martins. Silver nanoparticles (AgNPs) was purchased from Sigma Aldrich, reference 576832, lot MKBF5701V. The AgNPs particle sizes are in the range of 26–41 nm with 99.9% of purity originally coated with 0.1 wt% of PVP as a surfactant. The PVP (K90) (average molecular weight = 1,300,000 g mol^{-1}), was purchased from Plasdone.

Antioxidant Irganox®B215 ED, 67% tris(2,4-ditert-butylphenyl)phosphite and 33% pentaerythritol tetrakis[3-[3,5-di-tert-butyl-4-hydroxyphenyl]propionate] from BASF.

2.2. Methods

2.2.1. Radiation process

The irradiation process of the polymer pellets was carried at room temperature and at dose rate of 5 kGy h^{-1}, using a multipurpose ^{60}Co gamma irradiator. The polypropylene irradiation was performed at 12.5 kGy dose monitored by a Harwell Red Perspex 4034 dosimeter. After irradiation, the samples were heated for 1 h at 90 °C to promote the recombination and annihilation of residual radicals [25,26].

2.2.2. Preparation of the nanocomposites

The blend of iPP and PP 12.5 kGy (50/50 wt%) were mixed with Irganox® B 215 ED, long-term thermal stabilizer, in a rotary mixer for 12 h. The PP-nanocomposites were prepared by addition of AgNPs at different concentrations of 0.1%; 0.25%; 0.5%; 1.0%; 1.0% (PVP), 2.0% and 4.0% in wt%. The sample with 1.0% of AgNPs added with PVP as surfactant was mixed with ultrasonic mixer equipment, Quimis - Brazil, at 2000 rpm for 20 min. The polypropylene composite was processed in a twin-screw extruder (Haake co-rotating, Model Rheomex PTW 16/25), with the following processing conditions: the temperature profile (feed to die) was 180 to 195 °C, with a speed of 100 rpm. After mixing, the nanocomposites were granulated in a granulator Primotécnica W-702-3. The PP-AgNPs nanocomposite films were obtained by compression molding at 190 °C for 10 min without pressure and 5 min at a pressure of 80 bar, after that these films were cooled at room temperature before

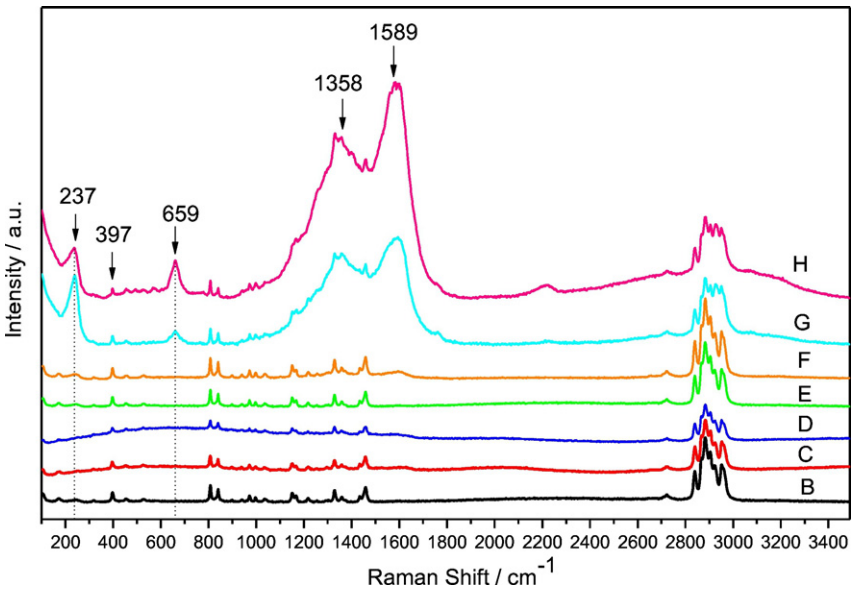

Fig. 1. Raman spectrum of polypropylene films with AgNPs: B) PP0.1% AgNPs; C) PP 0.25% AgNPs; D) PP 0.5% AgNPs; E) PP 1.0% AgNPs; F) PP 1.0% AgNPs PVP; G) PP 2.0% AgNPs; H) PP 4.0% AgNPs.

removing from the mold. Eight different samples of PP-nanocomposites were prepared and described in Table 1.

2.3. Characterization

2.3.1. Raman spectroscopy

Raman spectroscopic characterization were performed using the Raman laser microscope DXR ™ 720 nm, Thermo Scientific.

2.3.2. Scanning electron microscopy and energy-dispersive spectroscopy

The as prepared specimens were examined using a Hitachi TM3000, coupled with a Bruker Quantax 70 for the collection of energy dispersive X-ray (EDS) spectroscopic data. The EDS analysis was carried out at 15 keV and the acquisition period was 120 s.

2.3.3. Transmission electron microscopy

The morphology of the samples was examined with a JEOL JEM-2100 transmission electron microscope operating at voltage of 80 kV. Ultrathin sections (80 nm) were prepared with a Leica EM FC6 ultramicrotome with a diamond knife.

2.3.4. Differential scanning calorimetry

Thermal properties of specimens were analyzed using a Mettler Toledo DSC 822e differential scanning calorimeter. The thermal behavior of polymer nanocomposite films was obtained by: (1) heating from −50 to 280 °C at a heating rate of 10 °C min^{-1} under nitrogen atmosphere; (2) holding for 5 min at 280 °C, and (3) then cooling to −50 °C and reheating to 280 °C at 10 °C min^{-1}. Melting enthalpy value for 100% crystalline PP is 209 kJ kg^{-1} [27,28]. The percentage crystallinity of the polymer and polymer nanocomposite was calculated using the following Eq. (1):

$$X_c(\%) = \frac{\Delta H_f \times 100}{\Delta H_0} \quad (1)$$

2.3.5. Thermogravimetry analysis

Thermogravimetry curves were obtained with an SDTA 851 thermobalance (Mettler-Toledo), using samples of about 10 mg in alumina pans, under nitrogen atmosphere of 50 mL min^{-1}, in range from 25 up to 600 °C, at a heating rate of 10 °C min^{-1}.

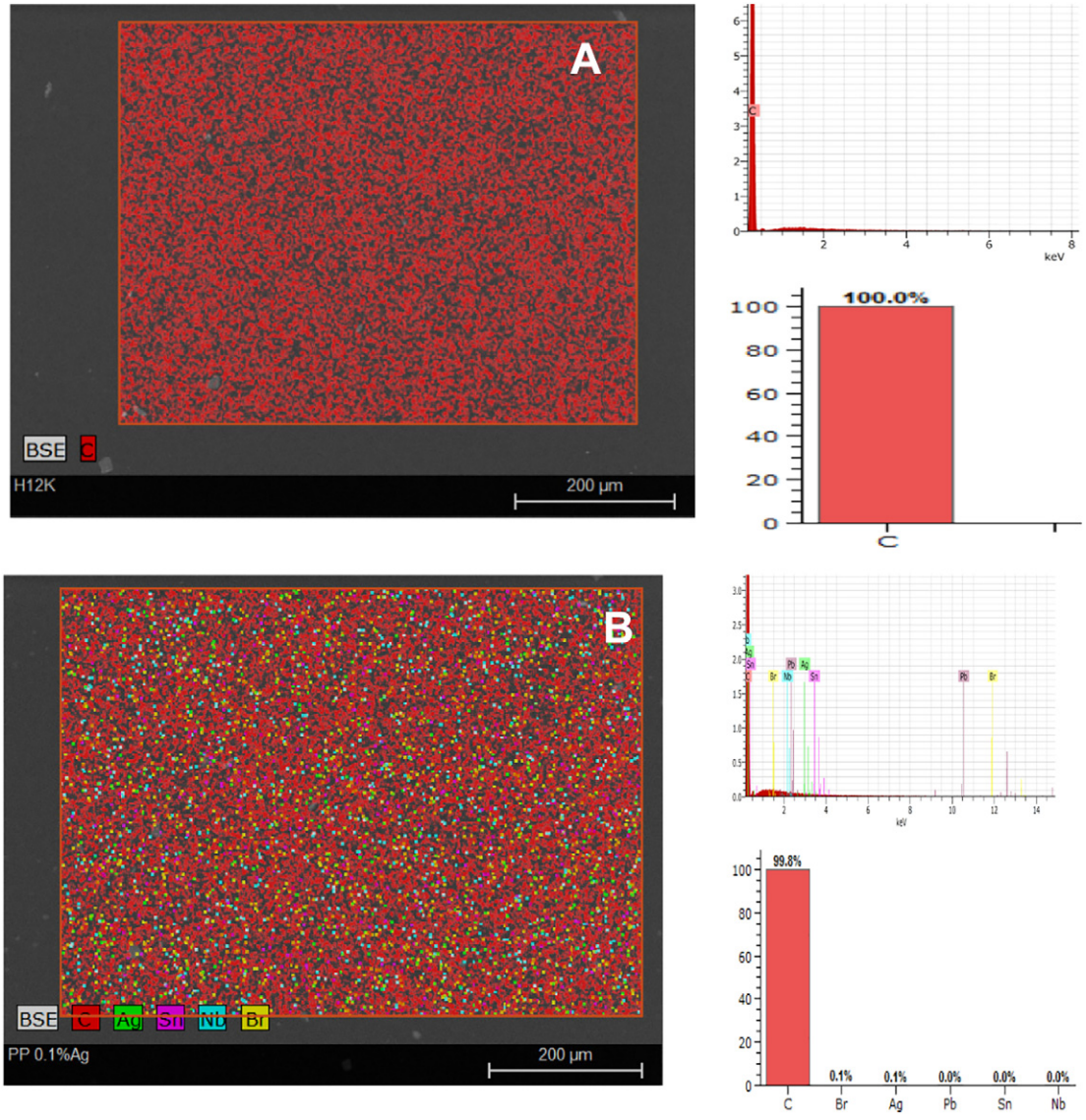

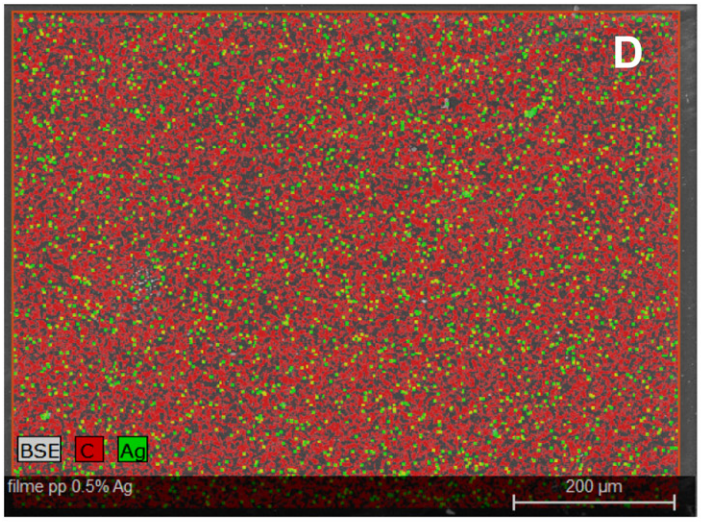
D
BSE
C
Ag
filme pp 0.5% Ag
200 µm

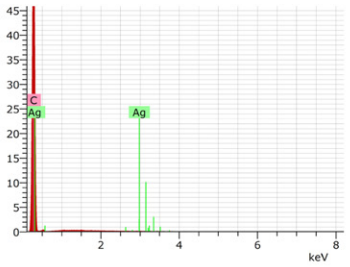
Ag
Ag
keV

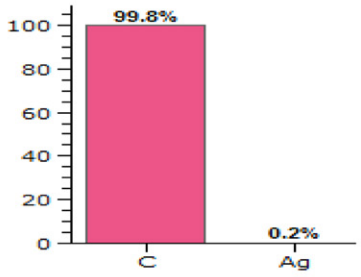
99.8%
0.2%
C
Ag

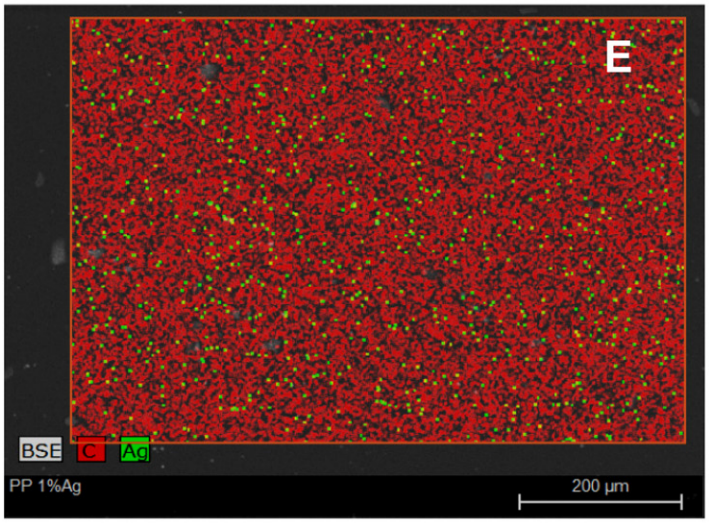
E
BSE
C
Ag
PP 1%Ag
200 µm

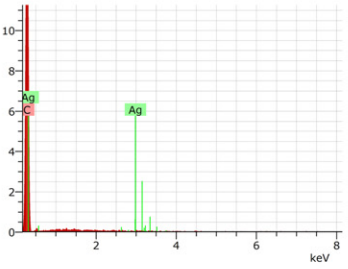
Ag
Ag
keV

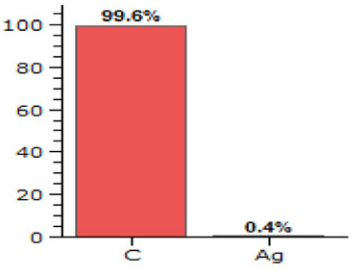
99.6%
0.4%
C
Ag

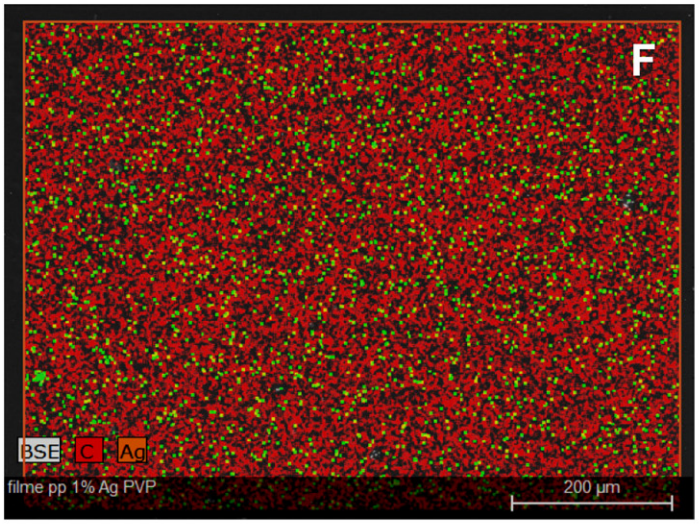
F
BSE
C
Ag
filme pp 1% Ag PVP
200 µm

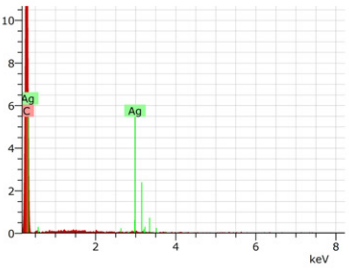
Ag
Ag
keV

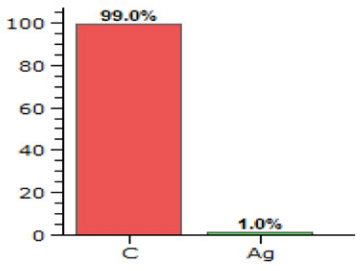
99.0%
1.0%
C
Ag

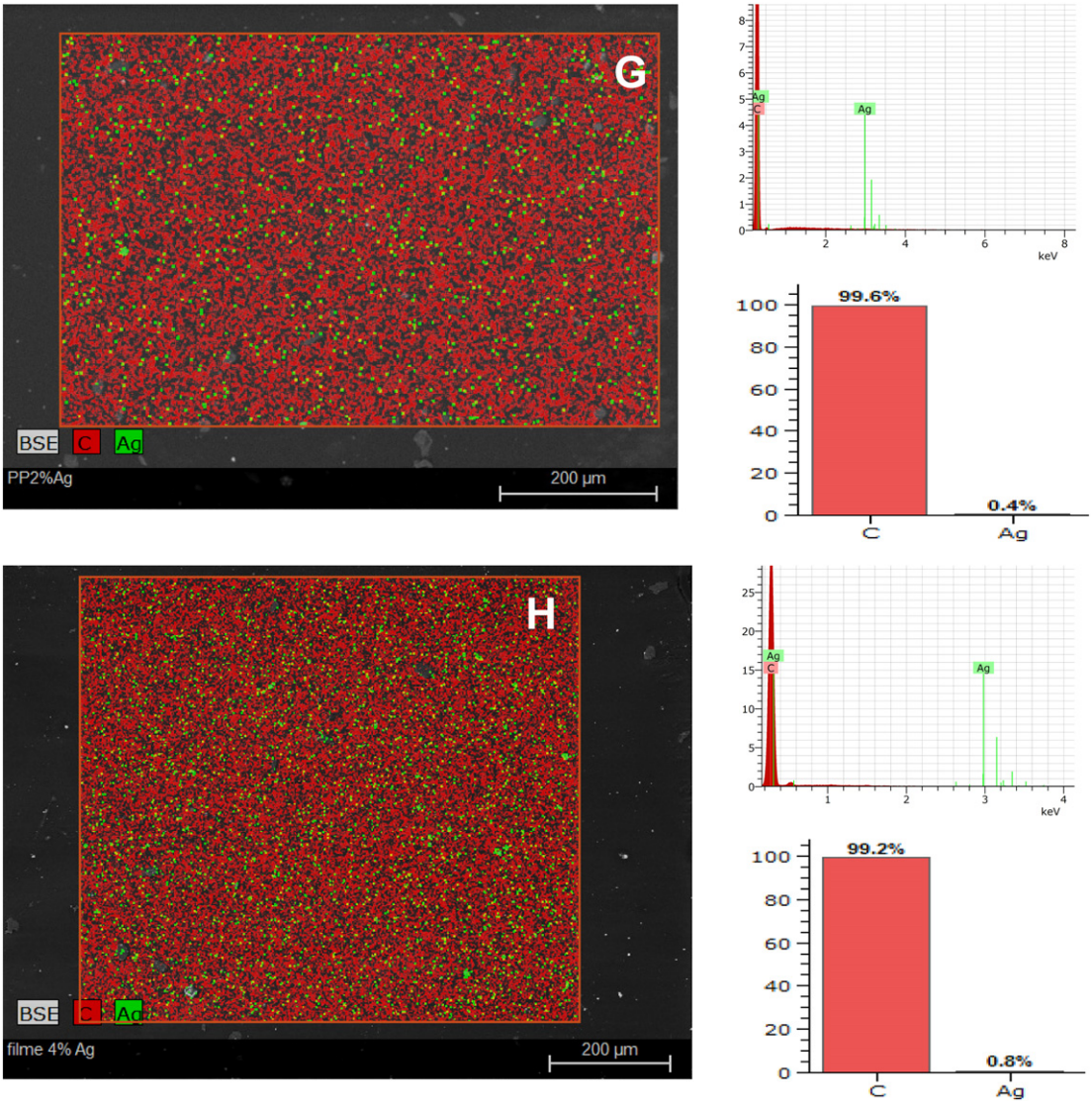

Fig. 2. SEM images and EDS mapping of Ag dispersed in the PP films: A) PP 0; B) PP 0.1% AgNPs; D) PP 0.5% AgNPs; E) PP 1.0% AgNPs; F) PP 1.0% AgNPs PVP; G) PP 2.0% AgNPs; H) PP 4.0% AgNPs.

2.3.6. X-ray diffraction

X-ray diffraction (XRD) measurements were carried out in the reflection mode on a Rigaku diffractometer Mini Flex II (Tokyo, Japan) operated at 30 kV voltage and a current of 15 mA with CuKα radiation (λ = 1.541,841 Å). Specimens were prepared with dimensions of (2.5 × 2.5 cm^2) and fixed on glass slides.

2.3.7. Mechanical test

The tensile tests were carried out on Zwick/Roell Z2.5 materials testing system equipped with TestXpert data acquisition system at 2.5 kN load. Thin films were cut according to the ASTM D882 standard in rectangular strip of 70 mm × 10 mm. Film thickness were ranged between 10 and 50 µm and was measured by the optical microscope. Samples at about, ten replicates, were tested for each film using separation grips of 50 mm. The cross-head speed was set at 0.01 mm s^{-1}. The tensile strength, modulus and toughness were determined by the TextXpert software.

2.3.8. Cytotoxicity test

The cytotoxicity assay, according to ISO 10993-5:2009 [29] was carried out with the exposure of NCTC L929 cell cultured in a 96 wells microplate to the extract obtained by the immersion of samples in cell culture medium, MEM (minimum Eagle's medium, Sigma Co., São Paulo, Brazil), for 24 h at 37 °C in a CO_2 humidified incubator. After this period, the medium was discarded and replaced with 0.2 mL of serially diluted extract of each sample (50; 25; 12.5; 6.25%). The cell line was acquired from American Type Culture Collection (ATCC) bank. The cytotoxicity effect was evaluated by neutral red uptake (NRU) methodology adapted according to previous work [30]. Samples of films in the square dimension of 2x2cm^2 were tested. Negative control used was non-toxic PVC pellets and positive control used was 0.02% phenol solution. Positive and negative controls were necessary to confirm the performance of the assay. Negative results implies in no cytotoxicity effect on human cells [31].

2.3.9. Antimicrobial susceptibility testing disk diffusion - Kirby-Bauer method

The objective of the test is to evaluate the AgNPs diffusion results contained in the polypropylene film, using standard procedures by NCCLS - National Committee for Clinical Laboratory Standards and ANVISA [32]. Bacteria and preparation of inoculum: Bacterial samples for testing were *P. aeruginosa* (Gram - negative) ATCC 25923 and *S. aureus* (Gram - positive) ATCC 27853. The colonies were suspended in nutrient medium (Mueller-Hinton) to obtain a concentration of 0.5 McFarland scale (1 × 10^8 CFU mL^{-1}). Agar was dispersed in the surface

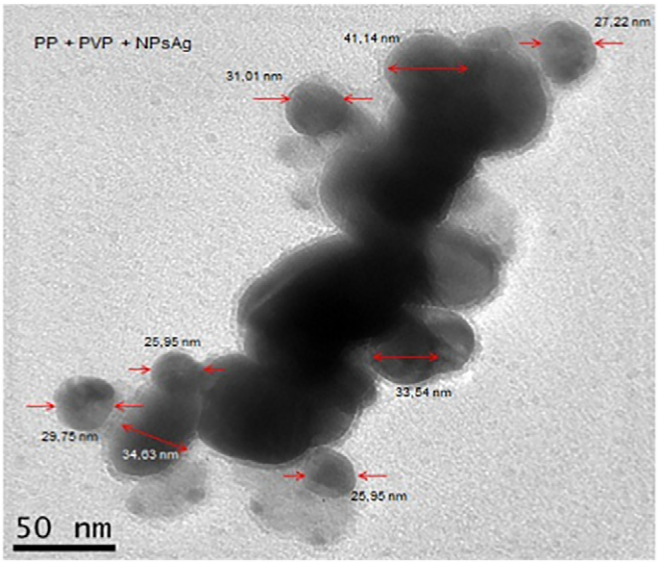

Fig. 3. TEM of polypropylene film with AgNPs PVP.

of a plate using a sterile cotton swab. After dried, samples with silver and the control (without silver) were individually added over the surface. The plates were incubated in bacteriological incubator at 37 °C for a period of 18 to 24 h. For a positive control we used the antimicrobial susceptibility testing of the same strains with antibiotic disc (CIP 5) Ciprofloxacin, when *P. aeruginosa* and *S. aureus* possess sensitivity. This methodology was used in polypropylene films with AgNPs. Test of bacteria proliferation was done with drops of bacteria solution (400 μL at 10^6 cell mL^{-1}) in contact with disks and after that dropped material is collected and tested for proliferation on Agar.

3. Results and discussion

3.1. Raman spectroscopy

The Fig. 1 shows the Raman spectrum of the nanocomposite films PP@AgNPs.

Raman spectroscopy of AgNPs was used in order to verify the functionalization groups associated with the stability of AgNPs. The Fig. 1 show a strong and sharp band at 237 cm^{-1} which was attributed to the stretching vibrations of Ag-O bond [33]. According to the literature [33,34], the range between 200 and 500 cm^{-1} is characterized by a broad band in which it is possible to define Raman shifts at 397 cm^{-1} spectrum attributed to Ag lattice vibration modes.

The broad and intense peaks at 1358 cm^{-1} and 1589 cm^{-1} were attributed to the enhancement of Raman lines by carbon polymeric segments absorbed on silver oxide [35,36]. The peak appearing at 659 cm^{-1} was attributed to the presence of PVP stabilized silver nanoparticles, as described by [37].

Table 2
DSC data of PP films during the second run of melting.

PP films	T_c/°C	$T_{m\beta}$/°C	$T_{m\alpha}$/°C	X_c/%
A) PP0	116.5	–	161.8	50.6
B) PP0.1%AgNPs	120.6	–	160.5	50.1
C) PP0.25%AgNPs	125.4	–	163.4	48.4
D) PP0.5%AgNPs	117.2	–	159.7	50.8
E) PP1%AgNPs	117.0	143.7	159.6	50.1
F) PP1%AgNPsPVP	120.9	148.5	161.6	47.5
G) PP2%AgNPs	116.7	145.0	159.5	50.2
H) PP4%AgNPs	116.5	148.0	163.3	44.2

3.2. Scanning electron microscopy and energy dispersive spectroscopy

The Fig. 2 shows the SEM images and EDS data for PP films with different percentages of silver nanoparticles. Semi-quantitative analysis of EDS data shows the increase of AgNPs content in the film, according to the formulation.

For elemental analysis of AgNPs were used in films with thickness ranging from 0.39 to 0.56 mm. The micrographs of the Fig. 2(A-H) showed red dots referring to carbon and green dots are clusters of silver nanoparticles. Fig. 2(A-H) also shows the EDS spectra in which peak observed at about 3.40 keV corresponds to the energy bands of AgL [38–42], which confirms the presence of silver. It was found on the surface of the films, homogeneous distribution of AgNPs and the presence of silver clusters in different regions. As semi quantitative determination of silver were found films with the following proportions: (0.1, 0.1, 0.2, 0.4, 1, 0.4, and 0.8%) of AgNPs in selected regions.

The use of PVP as surfactant showed better dispertion of the AgNPs and a more reliable result of Ag content.

3.3. Transmission electron microscopy

The TEM image of silver nanoparticles in polypropylene film is show in Fig.3.

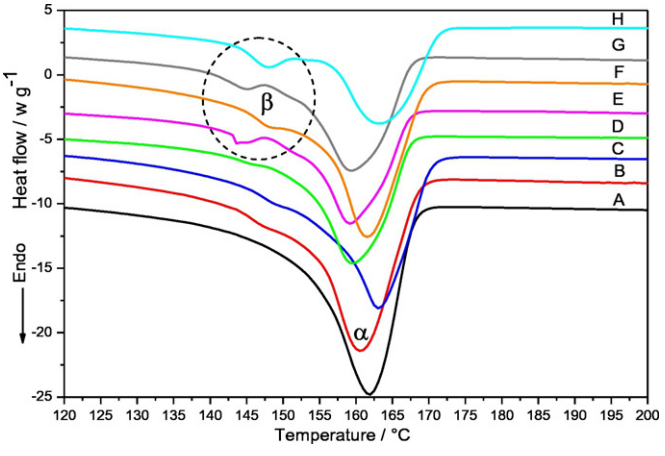

Fig. 4. DSC curves in the melting of the second heating run of films PP-AgNPs at different silver mass percentages: A) PP 0; B) PP0.1%AgNPs; C) PP 0.25% AgNPs; D) PP 0.5%AgNPs; E) PP 1.0%AgNPs; F) PP 1.0%AgNPsPVP; G) PP 2.0%AgNPs; H) PP 4.0%AgNPs.

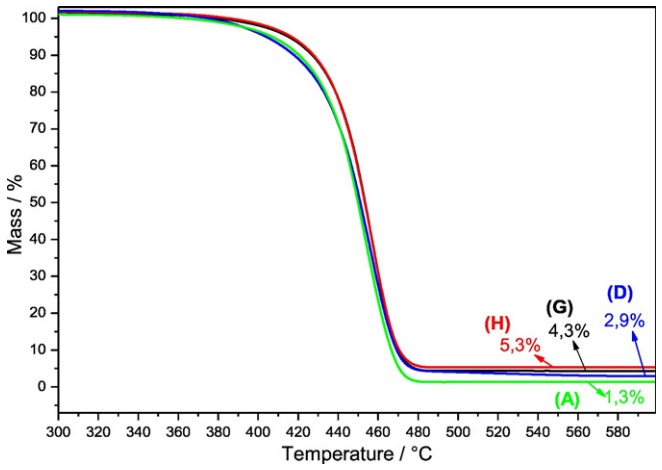

Fig. 5. TG decomposition curves of the AgNPs-polypropylene films. A) PP0; D) PP 0.5%AgNPs; G) PP 2.0%AgNPs and H) PP 4.0%AgNPs.

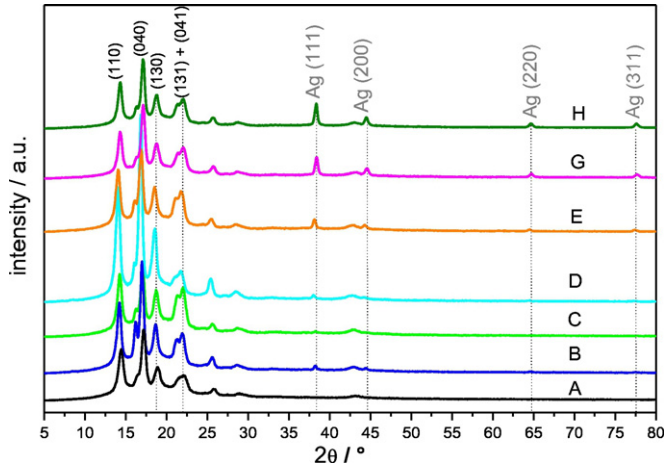

Fig. 6. X-ray diffraction in polypropylene nanocomposite films with AgNPs. A) PP 0; B) PP 0.1%AgNPs; C) PP 0.25%AgNPs; D) PP 0.5%AgNPs; E) PP 1.0% AgNPs; G) PP 2.0%AgNPs; H) PP 4.0%AgNPs.

TEM image of the silver nanoparticles from the polypropylene film matrix illustrates that spherical shapes of the silver nanoparticles with average size between 26 and 41 nm were measured in the polymer films.

3.4. Differential scanning calorimetry

The DSC reports are presented in Fig. 4. The curve corresponding to the PP films showed one melting peak, whereas two peaks are observed for AgNPs-polypropylene-films with percentages equal to or higher than that 1%AgNPs, samples E, F, G and H.

The DSC evaluated the crystallization temperature (T_C), temperature of second melting (T_{m2}), and the degree of crystallinity (X_C), and the results are presented at Table 2.

The nanocomposite shows, in Fig.4 a small peak in the region 143.7–148.5 °C followed by a strong peak in the region 159.5–163.4 °C. These two peaks represent the melting of the β-form and the α-form respectively. According to the literature [43–45] the melting temperature of the β-form is observed at around 145–150 °C. Compared to PP without AgNPs, the nanocomposites had, in some cases, one increase in crystallization temperature [45,46].

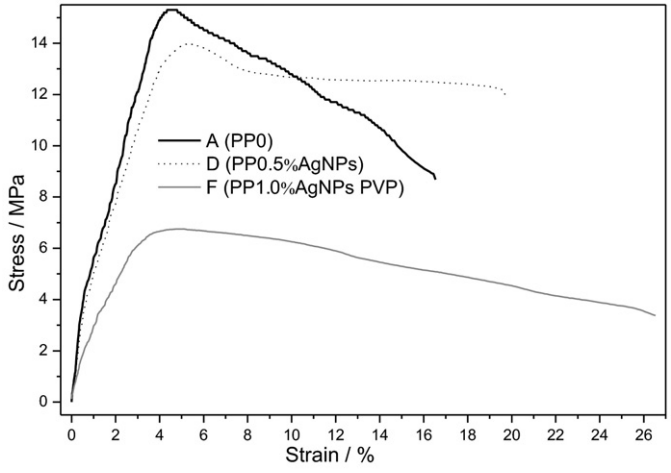

Fig. 7. Tensile strength test: comparison between the samples PP0; PP0.5%AgNPs and PP1.0%AgNPs PVP.

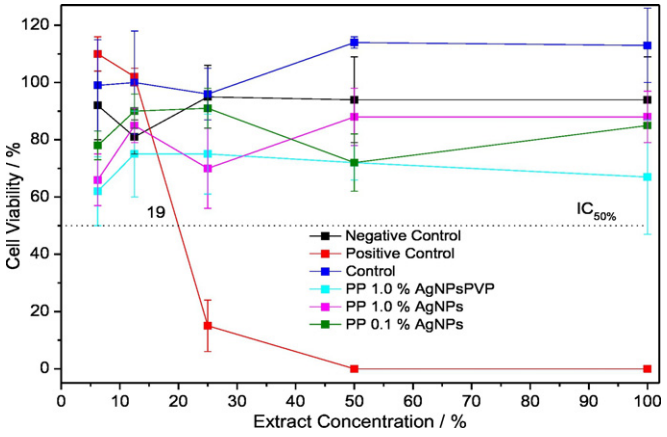

Fig. 8. Cell viability curves of polypropylene films containing: B) PP 0.1% AgNPs; E) PP 1.0% AgNPs; and F) PP 1.0%AgNPs PVP.

3.5. Thermogravimetry analysis

The TG results indicated decomposition of the samples, Fig. 5.

Thermograms of Fig. 5 show the decomposition of four polypropylene silver nanoparticles films. The PP0 film without AgNPs has 1.3% of residue since the PP film which 0.5% AgNPs was 2.9%, followed by PP film which 2%AgNPs was 4.3% and finally the film PP 4%AgNPs the residual value obtained was 5.3%.

The results confirm the presence of silver oxide residue in the films. However silver located internally in the films does not manifest the biocide activity, as evidenced in the tested samples of PP and PP 2%AgNPs, PP 4%AgNPs.

3.6. X-ray diffraction

Fig. 6 shows the XRD patterns of the nanocomposite films PP@ AgNPs.

The crystal structure and nature of AgNPs formed were analyzed by XRD. The XRD profiles show, in Fig. 6, characteristics peaks of scattering angles (2θ) of 38.1 and 44.3, 64.5 and 77.3 corresponding respectively to the (111), (200), (220) and (311) crystallographic planes. These diffraction peaks represent the face centered cubic (fcc) crystalline structure of metallic silver [47], respectively (JCPDS file n°. 00–004-0783). The intensity of the XRD peaks increases with silver nanoparticles (wt%) concentration.

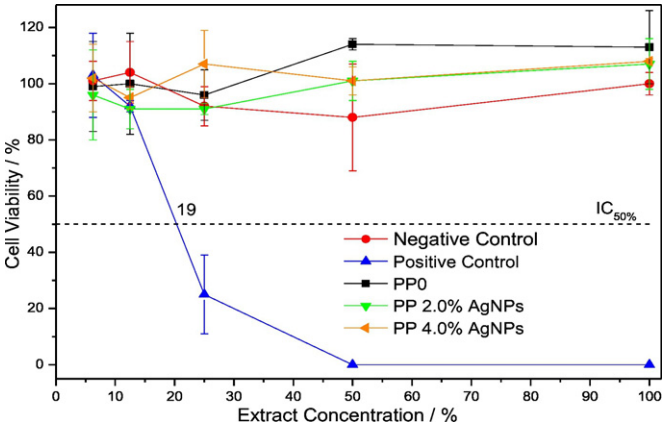

Fig. 9. Cell viability curves of polypropylene films containing: A) PP0; G) PP 2.0% AgNPs; and H) PP 4.0% of AgNPs.

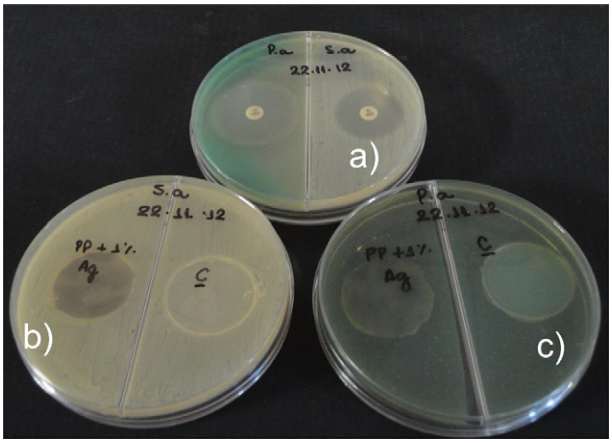

Fig. 10. Antimicrobials susceptibility test by diffusion disk in PP film 1%AgNPs specimen: a) Control with antibiotic (Ciprofloxacin) for *Pseudomonas aeruginosa* (*P. a.*) (left) and *Staphylococcus aureus* (*S. a.*) (right), both positive test; b) *S.a* test for PP 1%AgNPsPVP (left) and PP0 control without Ag (right); c) *P. a.* test for PP 1%AgNPsPVP (left) and PP control without Ag (right).

3.7. Mechanical test

A representative stress-strain-curve of nanocomposite films of the PPAgNPs is illustrated in Fig. 7.

An introduction of AgNPs into PP led to significant decrease of its tensile strength at nanoparticles content of 1%. However, polymer composite containing 0.5% of AgNPs showed similar value to the neat PP.

3.8. Cytotoxicity test

In this study, all the tested samples were noncytotoxic even at 100% extract concentration. They demonstrated similar behavior to negative control with non-cytotoxicity index ($IC_{50\%}$), as showed in Figs. 8 and 9.

Cell viability curves were obtained in a graphic with cell viabilities percentages against extract concentration. The cytotoxicity index $IC_{50\%}$ is obtained in the graphic and means the extract concentration which injures 50% of the cell population in the assay. The sample with cell viability curve above $IC_{50\%}$ line is considered noncytotoxic and under $IC_{50\%}$ line is considered toxic.

The cytotoxicity index was obtained by projecting a line from 50% cellular viability axis to extract concentration. All the lines are upper 50% cellular viability therefore, the films of AgNPs-PP are characterized as noncytotoxic by cell of mouse and in consequence noncytotoxic to human cells.

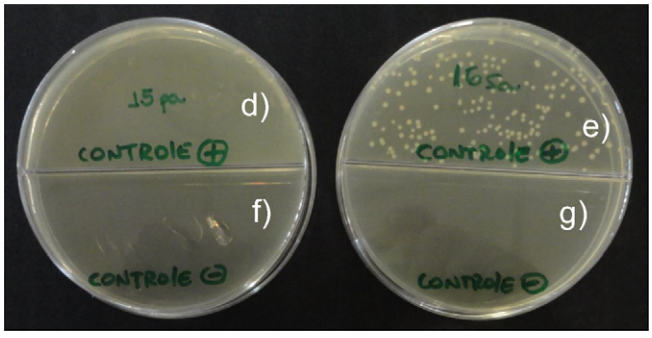

Fig. 11. Proliferation test on agar medium in PP0 (A) and 1%AgNPsPVP (F): d) dropped material in contact with PP0 surface tested for *P. a.* to agar; e) dropped material in contact with PP0 surface tested for *S. a.* to agar; f) in contact with PP1%AgNPsPVP tested for *P. a.*; g) in contact with PP1%AgNPsPVP tested for *S. a.*

3.9. Kirby-Bauer disk diffusion

Using disks PP 1% AgNPs samples diffusion tests (method of Kirby-Bauer) were done for *P. aeruginosa* and *S. aureus* in comparison with ciprofloxacin as positive control. As shown in Fig. 10 no halo formation was observed, hence no death of bacteria occurred.

The result suggests that there was no diffusion of silver to the culture medium. Test for proliferation were done for samples with drops of bacteria solution (400 μL at 10^6 cell mL^{-1}) in contact with disks of a) and f). The dropped material were removed after 2 h and cultured in agar, Fig. 11.

After the incubation time, the result shows the formation of colonies, both as d) *P. aeruginosa* and e) *S. aureus*, in samples of dropped bacteria solution taken from the PP surface. However material from disc surface PP1%AgNPsPVP showed no growth of any colonies indicating that the film with silver showed 100% biocide activity (f, g).

The mechanism for release of metal ions (Ag^+) is the corrosion of particles present in the bulk of the polymer owing to the diffusion of water molecules coming from the bacteria medium into the surface of particles [48].

Even highly non-polar matrices such as polyethylene or polypropylene allow the diffusion of water molecules and the polymer particle interface can further increase water diffusion through holes or micron-scale defects [49]. In the present results analyzed, the proliferation test showed contact bactericide activity. Taking into account the absence of clear zones of inhibition of test culture growth, is clear that the rate of silver ions diffusion is too low or even absent. Therefore, it can be proposed that PPAgNPs composites probably act as contact-active antimicrobial material without detectable biocide release.

4. Conclusion

This study was concentrated on the preparation of the films of PPAgNPs nanocomposites obtained by extrusion process. The used PVP surfactant, improves dispersion of nanosilver.

The TEM analysis verified the presence of silver nanoparticles clusters with size between 26 and 41 nm in the film. An introduction of AgNPs into PP led to significant decrease of its tensile strength at nanoparticles content of 1%. However, polymer composite containing 0.5% of AgNPs showed similar value to the neat PP.

Proliferation test for material in contact with surfaces of sample (F) (PP 1%AgNPsPVP) showed biocide activity to *P. aeruginosa* and *S. aureus* with 100% death of bacteria. The investigations of the cytotoxicity test in films were characterized as noncytotoxic by cell of mouse and in consequence noncytotoxic to human cells. Therefore, the presence of surfactant-coated silver nanoparticles allows antibacterial protection in contact-active without detectable biocide release.

Acknowledgement

The authors acknowledge financial support for this work from CAPES-Process: CSF-PVE's - 88887.115684/2016-00, CCTM/IPEN, for microscopy analysis (SEM and TEM), Sizue O. Rogero, laboratory biomaterials polymeric CQMA/IPEN, for the cytotoxicity tests, the technicians Mr. Eleosmar Gasparin and Nelson R. Bueno, for technical support and multipurpose gamma irradiation facility at the CTR/IPEN.

References

[1] H. Roder, O. Vogl, 17th international Herman F. Mark symposium: polypropylene – a material of the future, Prog. Polym. Sci. 24 (1999) 1205–1215.
[2] C.F. Ou, The crystallization characteristics of polypropylene and low ethylene content polypropylene copolymer with copolyesters, Eur. Polym. J. 38 (2002) 467–473.
[3] F.H. Su, H.X. Huang, Rheology and thermal behavior of long branching polypropylene prepared by reactive extrusion, J. Appl. Polym. Sci. 113 (2009) 2126–2135.
[4] K. Chikhalikar, A. Deshpande, H. Pol, D. Dhoble, S. Jha, K. Jadhav, S. Mahajan, Z. Ahmad, S. Kulkarni, S. Gupta, A. Lele, Long chain branched impact copolymer of polypropylene: microstructure and rheology, Polym. Eng. Sci. 54 (2014) 1–12.

[5] Y. Amintowlieh, C. Tzoganakis, S.G. Hatzikiriakos, A. Penlidis, Effects of processing variables on polypropylene degradation and long chain branching with UV irradiation, Polym. Degrad. Stab. 104 (2014) 1–10.
[6] W.L. Oliani, D.F. Parra, L.F.C.P. Lima, A.B. Lugao, Morphological characterization of branched PP under stretching, Polym. Bull. 68 (2012) 2121–2130.
[7] W.L. Oliani, L.F.C.P. Lima, D.F. Parra, D.B. Dias, A.B. Lugao, Study of the morphology, thermal and mechanical properties of irradiated isotactic polypropylene films, Radiat. Phys. Chem. 79 (2010) 325–328.
[8] H. Otaguro, B.W.H. Artel, D.F. Parra, E.C.L. Cardoso, L.F.C.P. Lima, A.B. Lugao, Polypropylene in the presence of trifunctional monomers and their influence in PP morphology, Polímeros: Ciência e Tecnologia 14 (2) (2004) 99–104.
[9] K. Makuuchi, S. Cheng, Radiation Processing of Polymer Materials and Its Industrial Applications. Chapter 8 – Long Chain Branching of Polymer Resins, Wiley, Canada, 2012 248–275.
[10] A.B. Lugao, H. Otaguro, D.F. Parra, A. Yoshiga, L.F.C.P. Lima, B.W.H. Artel, S. Liberman, Review on the production process and uses of controlled rheology polypropylene gamma radiation versus electron beam processing, Radiat. Phys. Chem. 76 (2007) 1688–1690.
[11] T. Sakai, Screw extrusion technology – past, present and future, Polymer 58 (2013) 847–857.
[12] D.W. Chae, B.C. Kim, Physical properties of isotactic poly(propylene)/silver nanocomposites: dynamic crystallization behavior and resultant morphology, Macromol. Mater. Eng. 290 (2005) 1149–1156.
[13] W.L. Oliani, L.F.C.P. Lima, S.O. Rogero, H.G. Riella, A.B. Lugao, D.F. Parra, AgNPs polypropylene gel films–thermal study and antibacterial-activity, J. Therm. Anal. Calorim. 119 (2015) 1963–1970.
[14] M. Fanelli, D.L. Feke, I.M. Zloczower, Prediction of the dispersion of particle clusters in the nanoscale. Part I. Steady shearing responses, Chem. Eng. Sci. 61 (2006) 473–488.
[15] M. Fanelli, D.L. Feke, I.M. Zloczower, Prediction of the dispersion of particle clusters in the nanoscale. Part II - unsteady shearing responses, Chem. Eng. Sci. 61 (2006) 4944–4956.
[16] M. Jokar, R.A. Rahman, N.A. Ibrahim, L.C. Abdullah, C. Pan, Melt production and antimicrobial efficiency of low-density polyethylene (LDPE) – silver nanocomposite film, Food Bioprocess Technol. 5 (2012) 719–728.
[17] P.J. Rivero, A. Urrutia, J. Goicoechea, C.R. Zamarreno, F.J. Arregui, I.R. Matías, An antibacterial coating based on a polymer/sol-gel hybrid matrix loaded with silver nanoparticles, Nanoscale Res. Lett. 6 (2011) 1–7.
[18] H. Palza, Antimicrobial polymers with metal nanoparticles, Int. J. Mol. Sci. 16 (2015) 2099–2116.
[19] C. Svitlana, E. Matthias, Silver as antibacterial agent: ion, nanoparticle, and metal, Angew. Chem. Int. Ed. 52 (2013) 1636–1653.
[20] E. Fages, J. Pascual, O. Fenollar, D. García-Sanoguera, R. Balart, Study of antibacterial properties of polypropylene filled with surfactant-coated silver, Polym. Eng. Sci. 51 (2011) 804–811.
[21] C. Marambio-Jones, E.M.V. Hoek, A review of the antibacterial effects of silver nanomaterials and potential implications for human health and the environment, J. Nanopart. Res. 12 (2010) 1531–1551.
[22] M. Rai, N. Duran, Metal Nanoparticles in Microbiology. Chapter 2 – An Insight Into the Bacterial Biogenesis of Silver Nanoparticles, Industrial Production and Scale-up, Springer, Berlin, 2011 17–35.
[23] T.V. Duncan, Applications of nanotechnology in food packaging and food safety: barrier materials, antimicrobial and sensors, J. Colloid Interface Sci. 363 (2011) 1–24.
[24] M. Ojeda, S. Tokumoto, A.L.D. Bracanca, L.F. Cassinelli, A.B. Lugao, B.W. Hutzler, Process for preparing high melt strength polypropylene and crosslinked prepared therewith. Patent Application Publication Pub. Nº. US (2004) (0171712 A1).
[25] W.L. Oliani, D.F. Parra, H.G. Riella, L.F.C.P. Lima, A.B. Lugao, Polypropylene nanogel: "myth or reality", Radiat. Phys. Chem. 81 (2012) 1460–1464.
[26] W.L. Oliani, D.F. Parra, D.M. Fermino, H.G. Riella, L.F.C.P. Lima, A.B. Lugao, Study of gel formation by ionizing radiation in polypropylene, Radiat. Phys. Chem. 84 (2013) 20–25.
[27] J.E. Mark, Physical Properties of Polymers Handbook, second ed. Springer, New York, 2007.
[28] C. Silvestre, M.L. Di-Lorenzo, E. Di-Pace, Crystallization of Polyolefins, in: C. Vasile (Ed.), Handbook of Polyolefins, 2rd ed.Marcel Dekker, New York, 2000.
[29] ISO 10993-5, Biological Evaluation of Medical Devices. Pat 5: Tests for In Vitro Cytotoxicity, 2009.
[30] G. Ciapetti, D. Granchi, E. Verri, L. Savarino, D. Cavedagna, A. Pizzoferrato, Application of a neutral red and amido black staining for rapid, reliable cytotoxicity testing of biomaterials, Biomaterials 17 (1996) 1259–1264.
[31] S.O. Rogero, S.M. Malmonge, A.B. Lugao, T.I. Ikeda, L. Miyamaru, A.S. Cruz, Biocompatibility study of polymeric biomaterials, Artif. Organs 27 (2003) 424–427.
[32] ANVISA – Agência Nacional de Vigilância Sanitária, Padronização dos Testes de Sensibilidade a Antimicrobianos por Disco-difusão. M2- A8, 23, n°1, 2003.
[33] I. Martina, R. Wiesinger, D. Jembrih-Simburger, M. Schreiner, Micro-Raman characterization of silver corrosion products: instrumental set up and reference database, e-Preservation Sci. 9 (2012) 1–8.
[34] S. Mohan, O.S. Oluwafemi, S.P. Songca, D. Rouxel, O. Joubert, N. Kalarikkal, S. Thomas, Synthesis, antibacterial, cytotoxicity and sensing properties of starch capped silver nanoparticles, J. Mol. Liq. 213 (2016) 75–81.
[35] N.R.C. Raju, K.J. Kumar, Photodissociation effects on pulsed laser deposited silver oxide thin films: surface enhanced resonance Raman scattering, J. Raman Spectrosc. 42 (2011) 1505–1509.
[36] J.A.A. Alfaro, S.S. Valdes, L.F.R. Valle, H.O. Ortiz, J.M. Nonell, A.P.P. Soto, R.I.N. Cespedes, Y.A.P. Mercado, F.A. Belmontes, Ultrasound irradiation coating of silver nanoparticles on ABS sheet surface, J. Inorg. Organomet. Polym. 23 (2013) 673–683.
[37] N. Perkas, M. Shuster, G. Amirian, Y. Koltypin, A. Gedanken, Sonochemical immobilization of silver nanoparticles on porous polypropylene, J. Polym Sci. A Polym. Chem. 46 (2008) 1719–1729.
[38] R.A. Afreen, E. Ranganath, Synthesis of monodispersed silver nanoparticles by *Rhizopus stolonifer* and its antibacterial activity against MDR strains of pseudomonas aeruginosa from burnt patients, Int. J. Environ. Sci. 1 (2011) 1582–1592.
[39] D.V. Quang, P.B. Sarawade, A. Hilonga, J.K. Kim, Y.G. Chai, S.H. Kim, J.Y. Ryu, H.T. Kim, Preparation of silver nanoparticles containing silica micro beads and investigation of their antibacterial activity, Appl. Surf. Sci. 257 (2011) 6963–6970.
[40] Y.H. Kim, D.K. Lee, Y.S. Kang, Synthesis and characterization of Ag and Ag-SiO_2 nanoparticles, Colloids Surf. A Physicochem. Eng. Asp. 257–258 (2005) 273–276.
[41] M.G. Guzman, J. Dille, S. Godet, Synthesis of silver nanoparticles by chemical reduction method and their antibacterial activity, Int. J. Chem. Biol. Eng. 2 (2009) 104–111.
[42] Q. Wei, D. Tao, B. Deng, F. Hung, Comparative studies of silver nanocomposite fibers, J. Ind. Text. 38 (2009) 1–8.
[43] K. Mezghani, P.J. Phillips, γ-Phase in propylene copolymers at atmospheric pressure, Polymer 36 (1995) 2407–2411.
[44] S.C. Tjong, S. Bao, Structure and mechanical behavior of isotactic polypropylene composites filled with silver nanoparticles, E-Polymers 139 (2007) 1–17.
[45] D. Hybiak, J. Garbarczyk, Silver nanoparticles in isotactic polypropylene (iPP). Part I. Silver nanoparticles as metallic nucleating agents for β-iPP polymorph, Polymer 59 (2014) 585–591.
[46] D.W. Chae, B.C. Kim, Physical properties of isotactic polypropylene/silver nanocomposites: dynamic crystallization behavior and resultant morphology, Macromol. Mater. Eng. 290 (2005) 1149–1156.
[47] R. Kakkar, E.D. Sherly, K. Madgula, D.K. Devi, B. Sreedhar, Synergetic effect of sodium citrate and starch in the synthesis of silver nanoparticles, J. Appl. Polym. Sci. 126 (2012) E154–E161.
[48] C. Damm, H. Munstedt, A. Rosch, The antimicrobial efficacy of polyamide 6/silver-nano- and microcomposites, Mater. Chem. Phys. 108 (2008) 61–66.
[49] T.M. Ton-That, B.J. Jungnickel, Water diffusion into transcrystalline layers on polypropylene, J. Appl. Polym. Sci. 74 (1999) 3275–3285.